ARTICLE

Mechanism of Photolytic Decomposition of N-Halamine Antimicrobial Siloxane Coatings

Hasan B. Kocer,[†] Akin Akdag,[‡] S. D. Worley,*[,‡] Orlando Acevedo,[†] R. M. Broughton,[†] and Yonnie Wu[‡]

Department of Polymer and Fiber Engineering and Department of Chemistry and Biochemistry, Auburn University, Auburn, Alabama 36849

ABSTRACT Generally, antimicrobial N-halamine siloxane coatings can be rehalogenated repetitively upon loss of their biocidal efficacies, a marked advantage over coatings containing other antimicrobial materials. However, the N-halamine materials tend to slowly decompose upon exposure to ultraviolet irradiation as in direct sunlight. In this work the mechanism of photolytic decomposition for the N-halamine siloxanes has been studied using spectroscopic and theoretical methods. It was found that the N-chlorinated coatings slowly decomposed upon UVA irradiation, whereas the unhalogenated coatings did not. Model compound evidence in this work suggests that upon UVA irradiation, the N−Cl bond dissociates homolytically, followed by a Cl radical migration to the alkyl side chain connected to the siloxane tethering group. An alpha and/or beta scission then occurs causing partial loss of the biocidal moiety from the surface of the coated material, thus precluding complete rechlorination. NMR, FTIR, GCMS, and computations at the DFT (U)B3LYP/6-311++G(2d,p) level of theory have been employed in reaching this conclusion.

KEYWORDS: antimicrobial materials • siloxanes • N-halamines • UVA irradiation • decomposition products

INTRODUCTION

It was established in the mid 1970s that N-halamines are excellent antimicrobial compounds for several reasons including biocidal efficacies, stabilities in aqueous solution and in dry storage, lack of corrosion of surfaces, low toxicities, and relatively low expense (1). Extensive work on these antimicrobial compounds for disinfection in aqueous solution was reported from these laboratories during the 1980s that illustrated their potential for use in a broad variety of applications (2). In the 1990s, the work was extended to N-halamine antimicrobial polymers for use in potable water disinfection (3−5) and antimicrobial textiles (6, 7). In more recent times, N-halamine materials have been developed and investigated extensively in several laboratories (8−11).

Antimicrobial N-halamine moieties have been attached to surfaces such as cellulose fibers by several grafting, tethering, and copolymerization methods. One of the more successful methods has been to bond the N-halamine precursor to a silane which can then tether to the surface through covalent ether linkages becoming a poly siloxane on the surface (see Figure 1). The first effort in this regard was the reaction of the potassium salt of 5,5-dimethylhydantoin with chloropropyltriethoxysilane, followed by curing onto cellulose fibers; chlorination with dilute household bleach then produced antimicrobial fibers which were capable of producing 6-log inactivations of *Staphylococcus aureus* and *Escherichia coli* O157:H7 within 10 min contact

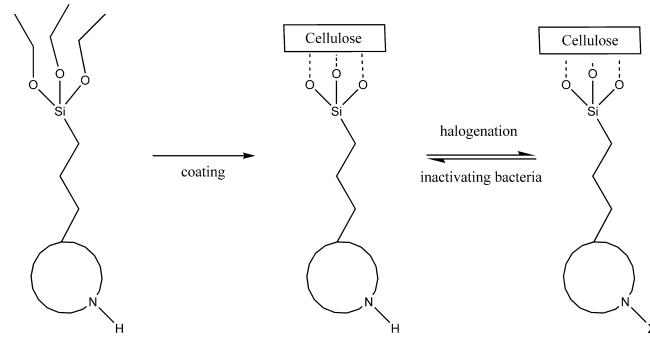

FIGURE 1. Preparation of siloxane antimicrobial coatings (X = Cl, Br).

and withstanding 50 machine washes without losing their biocidal efficacies (12). This material has been studied extensively in these laboratories, and although other derivatives have been subsequently developed (13−16), it remains the least expensive alternative, and it can be modified by copolymerization with a quat silane to render it soluble in water, a distinct advantage for use in the industrial sector (17). Also, recently it has been demonstrated to be effective in inactivation of chemical agents (18). However, there remains one limitation of the N-halamine siloxane materials, and thus far for most N-halamines in general: their stabilities to loss of halogen in sunlight (UV irradiation). Sandstrom and Sun have reported that aromatic structures can contribute to the absorption of UV radiation and thus shield the N−Cl bond from dissociation (19). They found that this was true for chlorinated Nomex when irradiated in the 315−400 nm range under very dry conditions at room temperature; however, when the experiment was conducted in a weathering chamber under controlled humidity and temperatures up to 50 °C, considerable decomposition was observed, and the lost chlorine could not be replenished (19). Based upon

* Corresponding author. Tel.: (334) 844-6980. Fax: (334) 844-6959. E-mail: worlesd@auburn.edu.
Received for review June 11, 2010 and accepted July 19, 2010
[†] Department of Polymer and Fiber Engineering, Auburn University.
[‡] Department of Chemistry and Biochemistry, Auburn University.
DOI: 10.1021/am100511x

Published on Web 07/29/2010

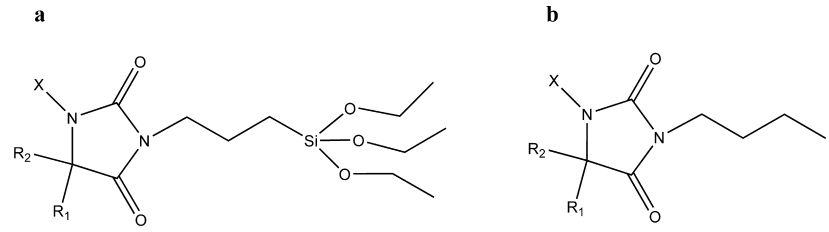

R_1 / R_2	X=H_2	X=Cl_2	X=H_2	X=Cl_2
Methyl / Methyl	MM	MM-Cl	MMm	MMm-Cl
Methyl / Phenyl	MP	MP-Cl	MPm	MPm-Cl
Phenyl / Phenyl	PP	PP-Cl	PPm	PPm-Cl

FIGURE 2. Structures of the synthesized siloxane coatings and the model compounds.

these observations, we performed a series of experiments in which the 5-methyl-5-phenyl- and 5,5-diphenyl- derivatives of 5,5-dimethylsilylpropylhydantoin (Figure 2) were coated onto cellulose and tested for biocidal efficacy against *Escherichia coli* O157:H7, evaluated for hydrolyses in washing tests, and preliminarily exposed to UVA irradiation in a weathering chamber. The results of these experiments, along with some model compound studies in which the silylpropyl moiety was replaced with a butyl group, demonstrated conclusively that phenyl substitution for these N-halamines actually weakened the amide N−Cl bond causing a destabilizing effect relative to the 5,5-dimethyl derivative (20). In this work, we have expanded the UV degradation studies and used NMR, FTIR, GCMS, and DFT computations in an attempt to determine the mechanism of the photodegradation process for the hydantoinylsilyl antimicrobial compounds.

EXPERIMENTAL SECTION

Materials. The triethoxysilylpropylhydantoin derivatives (MM, MP, PP, Figure 2A) were prepared according to the procedure described in our previous study (20). The structures of these derivatives were confirmed by ^{1}H and ^{13}C NMR. The three hydantoinyl siloxanes containing variations in methyl and phenyl group substitution at the 5 position of the hydantoin ring (shown as R_1 and R_2 in Figure 2A) were bonded to cellulose as described below.

Model compounds having n-butyl groups at the 3 position of the hydantoin ring (Figure 2B) were synthesized and characterized by ^{1}H and ^{13}C NMR as previously described (20).

Instrumentation. NMR spectra were obtained using a Bruker 250 spectrometer; ^{1}H (250 MHz) and ^{13}C (62.5 MHz) spectra were recorded with 16 and 1024 scans, respectively. A Bruker 400 spectrometer was employed to perform ^{1}H COSY and ^{1}H/^{13}C HMQC experiments to confirm assignments of structures. The FTIR data were obtained with a Nicolet 6700 FT-IR spectrometer with an ATR (Attenuated Total Reflectance) accessory, recorded with 32 scans at 2 cm^{-1} resolution. Mass spectra were obtained using LCMS (Waters Acquity UPLC and Q-Tof Premier) and GCMS (Waters GCT Premier) mass spectrometers.

Coating and Chlorination Procedures. Precursor silane monomers were first dissolved in an ethanol/water mixture (1:1 by weight) at concentrations ranging from 3 to 15 wt % so as to subsequently obtain chlorine loadings between 0.25 and 0.30%. The mixture was stirred for 15 min to produce a uniform solution. Cotton swatches (Style 400 Bleached 100% Cotton Print Cloth from Testfabrics, Inc., West Pittston, PA) were soaked in the solution for 15 min and then cured at 95 °C for 1 h. Then the swatches were soaked in a 0.5% detergent solution for 15 min, rinsed several times with water, and dried at room temperature. The coating solution employed containing the dissolved silane derivatives weighed 50 g, and the cotton swatches were cut into areas of 320 cm^2 each.

The treated fabrics were chlorinated by soaking in 10% household bleach (0.6% sodium hypochlorite) at pH 7 (adjusted with 6 N HCl) for 1 h. After rinsing with tap and distilled water, the swatches were then dried at 45 °C for 1 h to remove any unbonded chlorine from the material.

The precursor model compounds were chlorinated by a procedure similar to that described previously (9) and discussed in detail recently (20).

Analytical Titration. The chlorine concentrations loaded onto the coated samples and the model compounds were determined by the iodometric/thiosulfate titration method (20). The weight percent Cl^+ for the siloxane-coated samples and the model compounds were determined using eq 1.

$$Cl^+\% = (NV35.45)/(2W) \times 100\% \quad (1)$$

where $Cl^+\%$ is the weight percent of oxidative chlorine on the samples, N and V are the normality (equiv/L) and volume (L) of the titrant sodium thiosulfate, respectively, and W is the weight of the sample in grams. The purity of the chlorinated model compounds was determined to be 97−99%.

UVA Light Stability Testing. UVA light stability of the bound chlorine and the hydantoinyl siloxane coatings on cotton fabric samples was determined using an accelerated weathering tester (The Q-panel Company, Cleveland, OH). The samples were placed in the UV (Type A, 315−400 nm, 0.68 w/m^2 at 340 nm) chamber for contact times ranging up to 10 h. After specific times of exposure to UVA irradiation, the samples were removed from the UV chamber and titrated, or rechlorinated and titrated. UVA light irradiation of the chlorinated model compounds (MMm-Cl, MPm-Cl, and PPm-Cl, Figure 2B) was also performed in the accelerated weathering tester. In these studies, the samples as fine powders were dispersed in thin layers on glass slides. The chlorinated model compounds were exposed to UVA light for 120 h, a time chosen at which the bound oxidative chlorine was almost completely removed from the hydantoin moieties, and then immediately analyzed by NMR and mass spectroscopy techniques in an attempt to identify decomposition products. They were also titrated to determine whether any Cl^+ remained after the UVA exposure. The temperature was 37.6 °C, and the relative humidity was 17% during the UVA light irradiation.

Computational Studies. Density functional theory (DFT) computations at the restricted and unrestricted (U)B3LYP/6-311++G(2d,p) theory level (21, 22) were used to characterize the transition structures and ground states for the unchlorinated

Table 1. Effect of UVA Irradiation on the Hydantoinylsiloxane Coatings[a]

contact time (min)	wt % Cl^+ in MM-Cl	wt % Cl^+ in MP-Cl	wt % Cl^+ in PP-Cl
0	0.30	0.33	0.31
60	0.22	0.09	0.08
120	0.14	0.06	0.05
240	0.12	0.05	0.04
360	0.08	0.03	0.03

[a] Upon rechlorination after 360 min, the wt % Cl^+ in MM-Cl, MP-Cl, and PP-Cl became 0.22, 0.20, and 0.20, respectively.

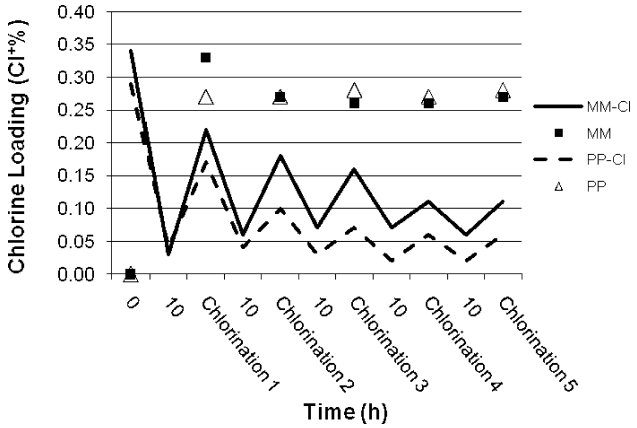

FIGURE 3. Stability toward repeated UVA light exposure of cotton coated with derivatized hydantoinyl siloxanes MM-Cl and PP-Cl (Cl^+% remaining) following a series of rechlorinations; the data for MM and PP represent chlorination after UVA exposure of the unchlorinated samples at the indicated UVA contact times.

and chlorinated butyl-substituted model compounds in vacuum using Gaussian 09 (23). The DFT calculations were used for geometry optimizations and computations of vibrational frequencies, which confirmed all stationary points as either minima or transition structures, and provided thermodynamic corrections. The complete basis set method CBS-QB3 (24) was also used to validate the B3LYP calculations. All calculations were performed on computers located at the Alabama Supercomputer Center.

RESULTS AND DISCUSSION

Stability toward Ultraviolet Light Irradiation of Hydantoinylsiloxane Coatings. Table 1 illustrates the stabilities of the hydantoinylsiloxane coatings on cotton toward UVA degradation. Several conclusions can be drawn from these data. First, all of the coatings lost oxidative chlorine upon exposure to UVA photons. Second, the phenyl derivatization did not stabilize the N—Cl bond; in fact, the effect was destabilization relative to that for MM-Cl for the two phenyl derivatives. It should be emphasized that the conditions of exposure in the Weathering Tester were not dry and at ambient temperature as noted by Sandstrom and Sun (19) in their studies of chlorinated Nomex. Third, none of the coatings could be completely rechlorinated after 360 min of UVA exposure, indicating that there was some decomposition of the structures of the hydantoinylsiloxane coatings. Further data are presented in Figure 3 that clearly indicate that the coatings are progressively decomposing over a 50 h contact time period, PP-Cl being slightly more

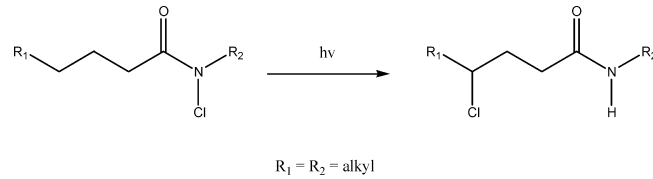

FIGURE 4. Intramolecular photorearrangement of acyclic N-halamides (1,5-hydrogen atom transfer).

prone to UVA photodegradation than was MM-Cl. It is notable that the chlorinated coatings did retain 0.05—0.12 wt % Cl^+ after five successive UVA exposures and rechlorinations, which would indicate that they remain capable of providing an antimicrobial function. However, the data shown in Figure 3 also demonstrate that the unchlorinated precursor coatings exhibited little or no significant decomposition in the presence of the UVA irradiation over the entire 50 h of exposure. Thus it is evident that the presence of chlorine bonded to the amide nitrogen is instrumental in the photodegradation process. This observation led us to an experimental and computational study of the model compounds mentioned above in order to attempt to elucidate the mechanism of photolytic decomposition for the hydantoinylsiloxane coatings.

Decomposition of Model Compounds under UVA Irradiation. It is well-known that N—Cl bonds can be cleaved either homolytically or heterolytically (25). In that studies here and elsewhere have clearly demonstrated that the N—Cl bonds in chlorinated hydantoins (and other N-halamines as well) are subject to dissociation in the presence of UV light, most probably in a radical process (9, 19, 20), we decided to perform a model compound study to see if the process is similar to a Hoffmann-Loeffler rearrangement (26—30).

For radical intermediates, Petterson et al. (26) reported a rearrangement of the chlorine atom on an acyclic N-chlorimide or acyclic N-chloramide from the nitrogen atom onto the acyl chain under UV irradiation (Hoffmann—Loeffler rearrangement). N-halamides having three or more methylene units in their acyl/alkyl side chains give rise to the Hoffmann—Loeffler rearrangement under UV irradiation, as shown in Figure 4 (26—29). The high selectivity for halogenation of C-4 in the acyl chain requires an intramolecular 1,5-hydrogen atom transfer from carbon to nitrogen involving a six-membered transition state; in some cases a 1,6 hydrogen transfer has been observed (27—30). When both N-alkyl and acyl chains of the N-halamide are small (less than three methylene units), a product of 1,4 hydrogen transfer also has been observed (30).

Although the reported examples were for chlorinated acyclic amides and imides, a similar intramolecular photolytic rearrangement might occur for the 1-chloro-3-alkyl-substituted hydantoin ring. The chlorine atom might migrate onto the alkyl chain at C-8 (1,6-hydrogen atom transfer) or C-7 (1,5-hydrogen atom transfer) (Figure 5) providing products A and B, respectively. Products A and B could further decompose by dehydrohalogenation processes.

To test this assumption, we irradiated the chlorinated model compounds with UVA light for 120 h, and FTIR, NMR,

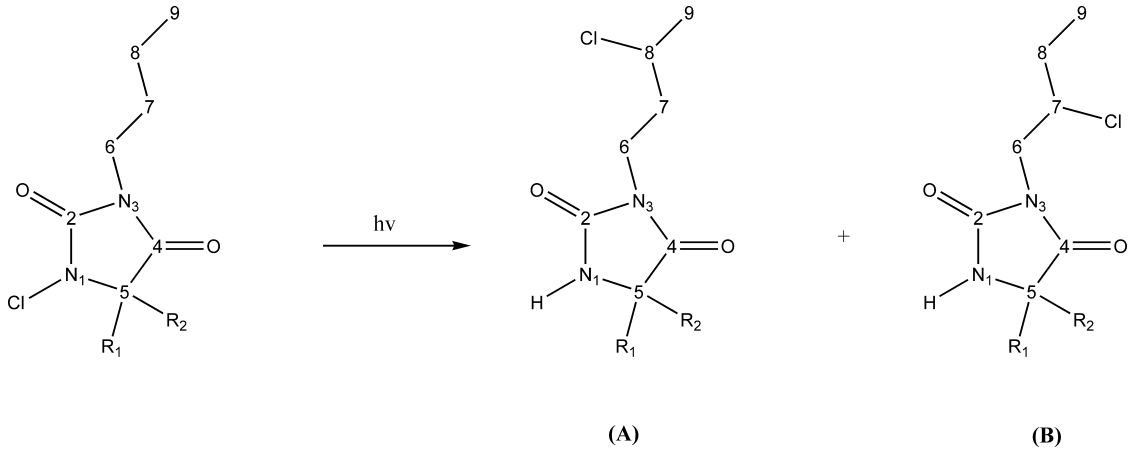

FIGURE 5. Possible photolytic rearrangements for 3-butyl-1-chlorohydantoins.

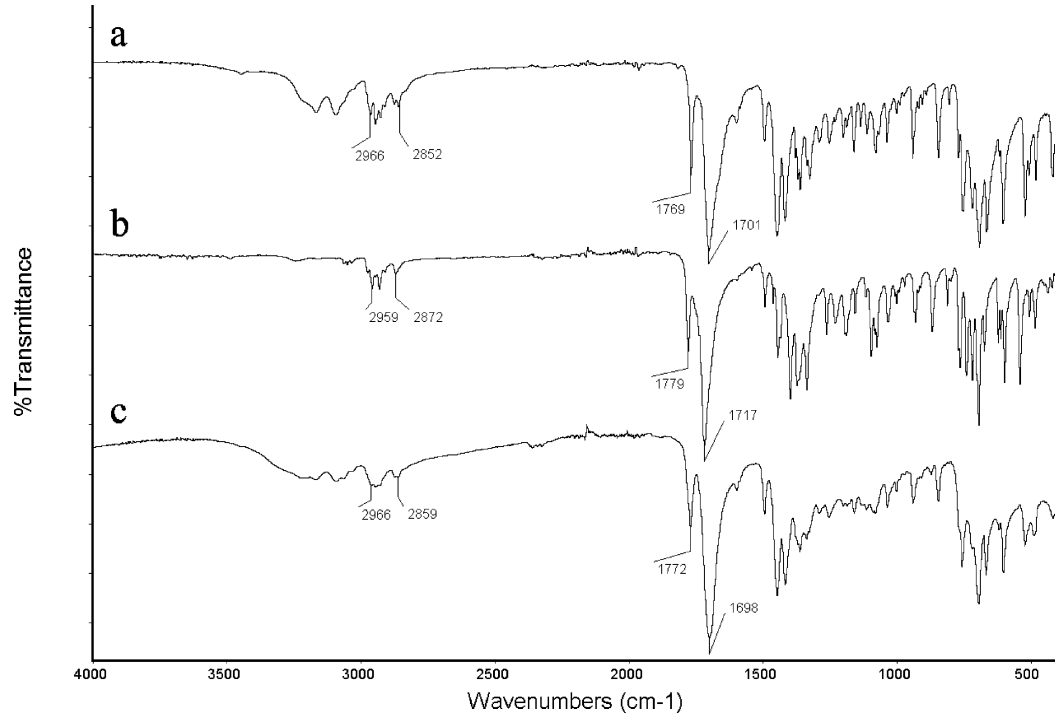

FIGURE 6. FTIR Spectra of (a) MMm, (b) MMm-Cl, and (c) UVA-irradiated MMm-Cl.

and mass spectrometry were employed to evaluate structural changes occurring during the photodecomposition.

FTIR Spectroscopy. The FTIR spectra of MMm, MMm-Cl, and UVA light- irradiated MMm-Cl are presented in Figure 6. The N−H stretching band at about 3300 cm^{-1} for MMm disappears upon chlorination to form MMm-Cl and reappears after UVA light irradiation, indicating partial reformation of the N−H bond. The strong bands at 1698−1701 and 1769−1772 cm^{-1} are attributable to carbonyl stretching vibrational modes for the hydantoin ring. These bands shifted to higher wavenumbers upon chlorination because of disruption of hydrogen bonding, and then shifted back to their original positions after exposure to UVA light. Several bands between 2800−3000 cm^{-1} due to stretching modes for methylene (CH_2) units lost some intensity after exposure to UVA light indicating that some structural changes occurred in the 3-butyl group during the UVA light irradiation of the chlorinated model compound. These observations are consistent with the titration data from above, i.e., slow decomposition of the model compound, but primarily just rupture and reformation of the N−Cl bond.

NMR Spectroscopy. Figure 7 shows the ^1H NMR spectra of MMm and MMm-Cl exposed to UV light for 120 h. There are not any ^1H NMR signals that can be assigned to MMm-Cl in the spectrum for the UVA-irradiated compound, indicating that all of the N−Cl bonds were broken (a broad signal at 7.30 ppm, which disappears upon chlorination and which is not shown in Figure 7, can be assigned to resonance of the amide proton of MMm). Therefore, a comparison between the NMR spectra of MMm and irradiated MMm-Cl samples would be best for investigating the structural changes. There are obviously several additional signals after UVA irradiation, demonstrating that there occurred structural changes in the chlorinated model compound during the irradiation process. First, the ratio between the integrated areas of the signals for the three methyl protons of C-9 at

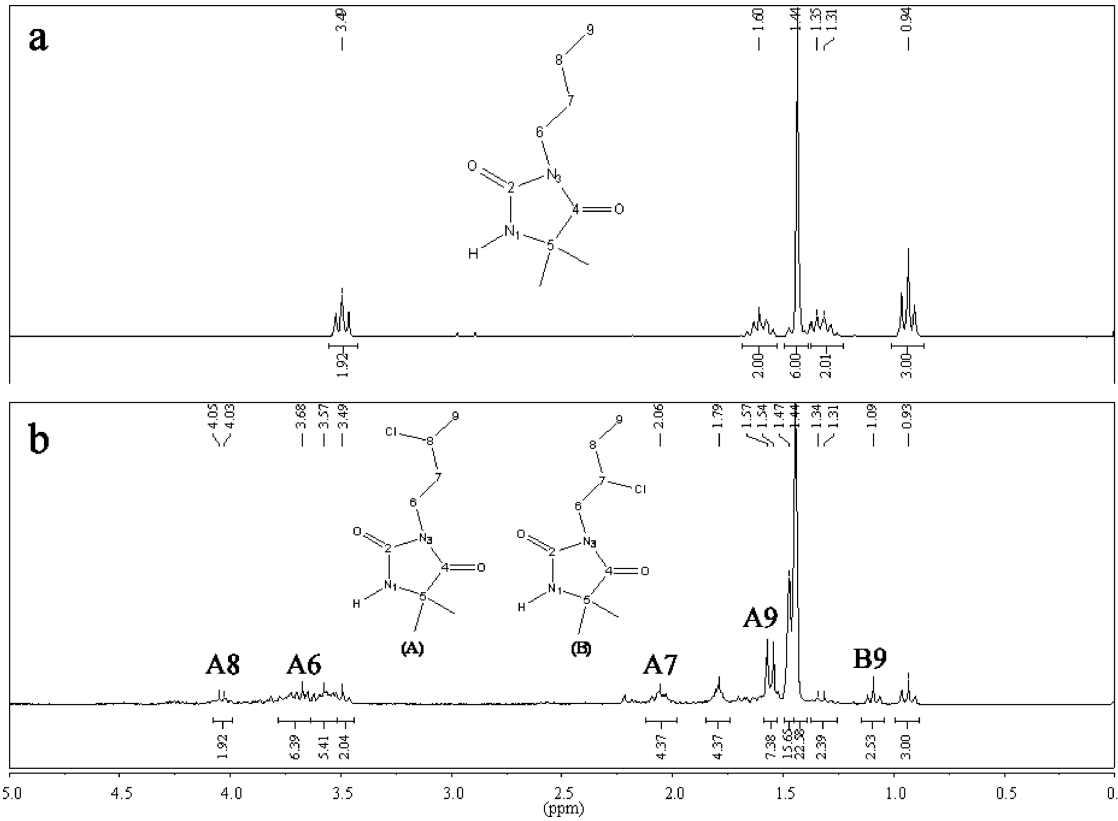

FIGURE 7. ^{1}H NMR spectra of (a) MMm and (b) UVA-irradiated MMm-Cl; the solvent was $CDCl_3$.

0.94 ppm to the six methyl protons at the 5 position of the hydantoin ring at 1.44 ppm was reduced to 3/38 after irradiation, indicating that there were structural changes on the n-butyl group attached at the 3 position of the hydantoin ring. The most intense additional signal is a doublet at 1.55 ppm that can be assigned to resonance of the product A (Figure 7b) methyl group protons (C-9). The signal at 4.03 ppm can be assigned to the product A C-8 proton (HC-Cl), while the bands at 2.06 ppm and 3.68 ppm can be assigned to product A C-7 and C-6 protons, respectively. There was also some product B in the UVA-irradiated sample to which the triplet at 1.09 ppm can be assigned for the methyl protons of Product B (C-9), while other proton signals for the product B are masked by product A signals, as product A appears to be the major product in the mixture. The signal assignments were confirmed by ^{1}H COSY and ^{1}H/^{13}C HMQC NMR experiments. Similar results affording the same conclusions were obtained upon comparing the ^{1}H NMR spectra of MPm and PPm with those of irradiated MPm-Cl and PPm-Cl, respectively (see the Supporting Information section).

Figure 8 shows the ^{13}C NMR spectra of MMm and MMm-Cl exposed to UVA light for 120 h. There are several additional signals observed in the UVA-irradiated sample. C-8 of the product A (HC-Cl) exhibited a signal at 55.8 ppm. Signals for resonances for other carbon atoms of the product A are observed at 25.5, 36.3, and 38.1 ppm, which can be assigned to C-9, C-7, and C-6, respectively. A resonance for the methyl carbon atom of the product B (C-9) was observed at 10.7 ppm, whereas B-8, B-7, and B-6 carbon atom signals were observed at 28.7, 60.5, and 44.2 ppm, respectively. Thus the ^{13}C and ^{1}H NMR data are in accord that products A and B result upon irradiation of MMm-Cl. Analogous results were observed for MPm and PPm relative to irradiated MPm-Cl and PPm-Cl, respectively, from their ^{13}C NMR data (see the Supporting Information).

Mass Spectrometry. Mass spectrometry data also supported the photo rearrangement of the chlorine atom to the alkyl side chain (Figure 9). The parent peak for MMm was measured as 184.12 g/mol (theoretical value is 184.12 g/mol) with GCMS; the mass of MMm-Cl could not be measured by GCMS because the N—Cl bond dissociated at a temperature lower than that (ca. 200 °C) (20) necessary for volatilization of the compound. However, ESI (electrospray ionization with formic acid) was used to measure a molecular weight of protonated MMm-Cl of 219.09 g/mol, indicating a value of 218.08 g/mol in agreement with the theoretical value for MMm-Cl. The chlorinated model compound MMm-Cl was exposed to UVA light for 120 h and then subjected to GCMS analysis. The GC of the UVA-irradiated MMm-Cl contained additional peaks in the chromatogram other than the starting material MMm. Figure 9 shows the Mass spectra of MMm and UVA-irradiated MMm-Cl. Surprisingly, the irradiated MMm-Cl exhibited a parent peak at 218.08 g/mol, which is the same molecular weight as for MMm-Cl. However, we were not able to observe this peak with MMm-Cl in a standard GCMS experiment since the N—Cl bond dissociated at lower temperature than that necessary for volatilization of the compound. Therefore, this peak must be assigned to a parent ion of a rearranged

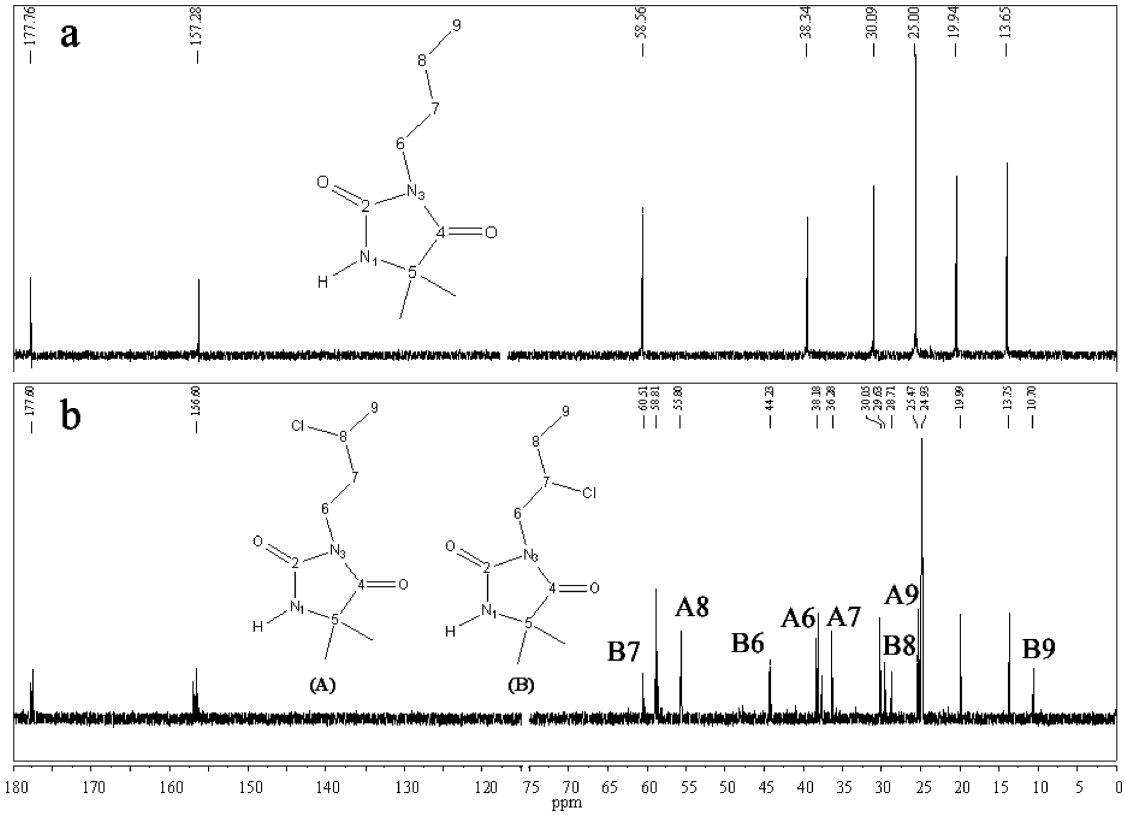

FIGURE 8. ^{13}C NMR spectra of (a) MMm and (b) UVA-irradiated MMm-Cl; the solvent was $CDCl_3$.

product such as product A or product B (Figure 5), structural isomers of MMm-Cl having strong C−Cl bonds. In addition, the base peak at 182.11 g/mol can be assigned to the dehydrohalogenation products of product A and product B. Similar results were also obtained from the mass spectral data for PPm-Cl (see the Supporting Information).

Thus for the model compounds, both NMR and mass spectrometry data support the transfer of the chlorine atom from the amide nitrogen of the hydantoin ring to C-6 and/or C-7 on the n-butyl chain, which could be effected by a photoinduced homolysis to produce amide and Cl radicals, followed by 1,5 or 1,6 hydrogen atom transfers through six- or seven-membered transition states.

Theoretical Computations. Quantum mechanical (QM) calculations at the (U)B3LYP/6-311++G(2d,p) level of theory were performed to assist in the elucidation of the mechanism of the photodegradation process for the hydantoinylsiloxanes. The same computational methodology was used in our recent study of MMm-Cl and PPm-Cl structures (20), and good agreement was found with reported bond distances, angles, and torsional values from X-ray crystallographic studies. Those calculations also attributed the selective shielding of the *ortho* protons in the experimental ^1H NMR spectrum of PPm-Cl to an induced twist in phenyl substituents caused by the chlorine atom at the N_1 position (20). Computations have been performed in the present study to explore the energetics and stabilities of the hydantoin compounds as related to the proposed mechanistic pathway of the photodegradation process as suggested above for the model compounds. In the first step, exposure to UVA light initiates the homolytic bond cleavage between N_1−Cl in MMm-Cl and PPm-Cl. To quantify this homolytic dissociation, we used the UB3LYP/6-311++G(2d,p) level of theory to compute the heats of formation ($\Delta_f H°_{298}$) for the radical Cl, PPm, and MMm species, and their corresponding bond dissociation enthalpies (BDE) were obtained using eq 2. The calculations predicted BDEs of 50.5 and 48.7 kcal/mol for MMm-Cl and PPm-Cl, respectively (Table 2). The experimental BDE at 298K for the NCl molecule is 62 kcal/mol (31), and a computed value of 60 kcal/mol for H_2N−Cl at the rigorous G3 level (32) places the current calculations for the amide-Cl BDE within a reasonable range.

$$BDE_{298} = \Delta_f H^0_{298}(\text{hydantoin}\bullet) + \Delta_f H^0_{298}(\text{Cl}\bullet) - \Delta_f H^0_{298}(\text{hydantoin-Cl}) \quad (2)$$

Furthermore, the computations predict that the MMm-Cl and PPm-Cl structures with a Cl bound at the N_1 position are more than 30 kcal/mol less stable than are the systems with a Cl bound to the butyl chain, suggesting a large thermodynamic driving force for the rearrangements. The computed relative enthalpies for the MMm-Cl and PPm-Cl gas-phase structures, where the Cl is covalently bonded at the N_1, C-7, and C-8 positions of the molecule (Figure 5), are summarized in Table 3. Calculations performed for MMm-Cl at the highly accurate CBS-QB3 level of theory confirmed the DFT findings in Table 3 (values in parentheses).

A subsequent intramolecular 1,5- or 1,6-hydrogen atom transfer from the C-7 or C-8 position to the N_1 atom is then

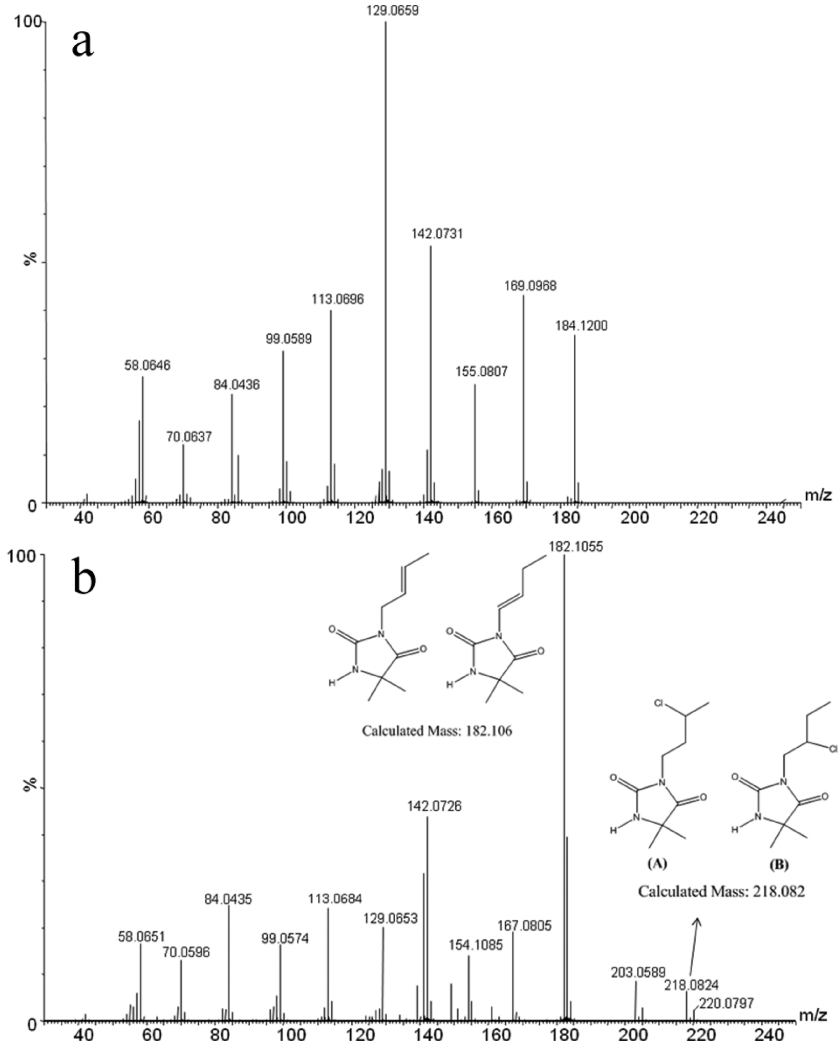

FIGURE 9. GCMS spectra of (a) MMm and (b) UVA-irradiated MMm-Cl.

Table 2. Calculated Bond Dissociation Enthalpy (BDE) for the N_1−Cl Bond in MMm-Cl and Activation Enthalpies, $\Delta H^{\ddagger}$, for the 1,5- and 1,6-Hydrogen Atom Transfers in the MMm Radical[a]

	BDE (N_1−Cl)	$\Delta H^{\ddagger}$ (1,5-H)	$\Delta H^{\ddagger}$ (1,6-H)
MMm	50.5	52.9	38.2

[a] Enthalpies (in kcal/mol) computed at the UB3LYP/6-311++G (2d,p) level of theory. 1,5-Hydrogen atom transfer between atoms C-7 and N_1 and 1,6-hydrogen atom transfer between atoms C-8 and N_1. Numbering scheme given in Figure 5.

Table 3. Calculated Gas-Phase Relative Enthalpies, ΔH (kcal/mol), for the Chlorinated Hydantoin Mimics[a]

	N_1−Cl	C-7-Cl	C-8-Cl
MMm-Cl	33.1 (32.2)	1.1 (0.0)	0.0 (0.4)
PPm-Cl	34.8	1.5	0.0

[a] Relative enthalpies computed at the B3LYP/6-311++G(2d,p) level of theory. Values in parentheses computed at the CBS-QB3 level of theory. Numbering scheme for the model compounds given in Figure 5.

proposed to proceed via a six- or seven-membered transition state, respectively, for the radical MMm species. The MMm transition structures were computed using the same DFT methodology, and the C−H and H−N breaking/making bond distances were predicted to be similar for both 1,5- and 1,6-hydrogen atom transfers with values of 1.43 and 1.30 Å and 1.44 and 1.29 Å, respectively (Figure 10). Despite the geometric similarities, the activation enthalpies differed significantly with an activation barrier for the 1,6-hydrogen atom transfer that was lower by 14.7 kcal/mol compared to the 1,5-hydrogen atom transfer (Table 2). The calculations are consistent with the present NMR data that find the UVA light-irradiated MMm-Cl compound with the Cl bound at the C-8 position to be the major product (Figure 7).

Loss of Antimicrobial Efficacy. Upon loss of the tethered hydantoin moiety from a surface, the antimicrobial property can no longer be regenerated by rechlorination. Thus the experimental observations in this work can only be retionalized by a final decomposition step in the mechanism. Once the Cl atom has covalently bonded to the resultant C-7 or C-8 radical atom, then the final step of the proposed photodecomposition mechanism can occur. The chlorine located at the alpha or beta position to the silicon atom, i.e., C-8 or C-7, could be simultaneously transferred to the silicon atom of the siloxane group accompanied by cleavage of the alkyl chain. Transition states

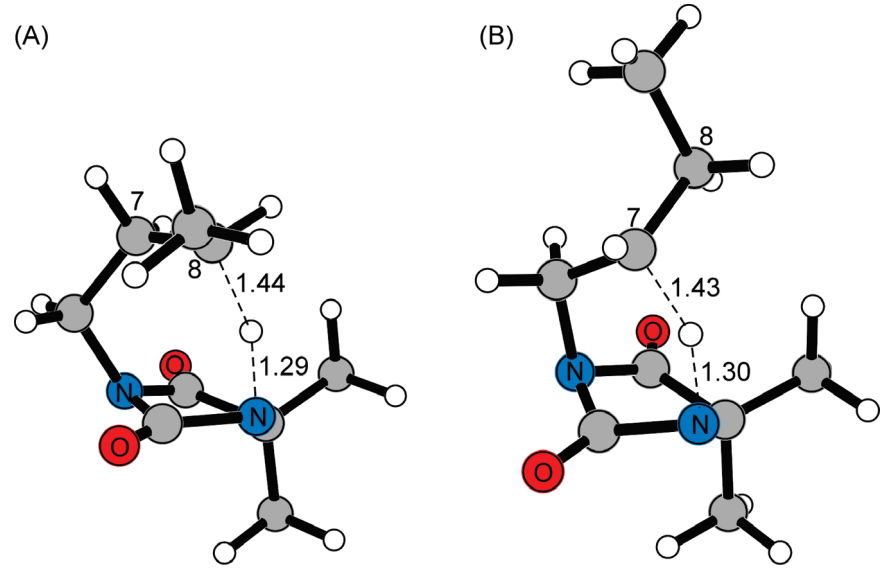

FIGURE 10. Transition structures at the UB3LYP/6-311++G(2d,p) level of theory for the 1,6- and 1,5-hydrogen atom transfer between atoms (A) C-8 and N_1 and (B) C-7 and N_1 in the MMm radical (distances in angstroms).

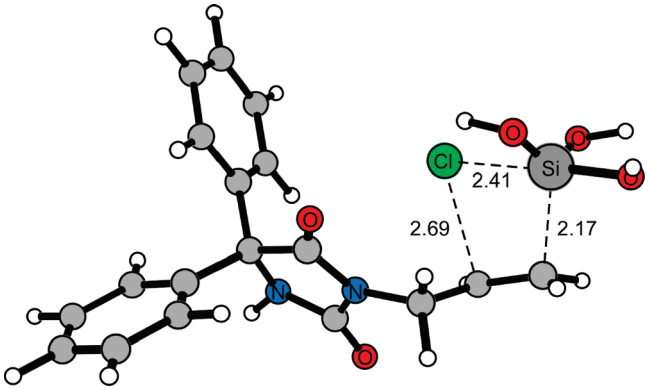

FIGURE 11. Transition structure at the UB3LYP/6-311++(2d,p) level of theory for the cleavage of the 7-chloro-5,5-diphenylhydantoin siloxane model (PPSi-Cl).; distances in angstroms.

Table 4. Activation Enthalpies (kcal/mol) for the 7-Chloro-5,5-dimethyl- and 7-Chloro-5,5-diphenyl-hydantoin Siloxane Mimic Transition Structures (MMSi-Cl and PPSi-Cl) from UB3LYP/6-311++G(2d,p)

	MMSi-Cl	PPSi-Cl
$\Delta H^{\dagger}$	33.9	34.8

have been computed for the beta position cleavage of the 7-chloro-5,5-dimethyl- and 7-chloro-5,5-diphenylsilylpropylhydantoins mimics, MMSi-Cl and PPSi-Cl, respectively, where the covalent ether linkages to the cellulose surface are replaced with hydrogen atoms for simplicity (Figure 11). In the activated complex the reaction occurs in a concomitant fashion where the Cl—C bond is breaking at 2.71 and 2.69 Å for MMSi-Cl and PPSi-Cl, respectively, the Cl—Si bond is forming at 2.42 and 2.41 Å for MMSi-Cl and PPSi-Cl, respectively, and the Si—C bond is breaking at 2.17 Å for both compounds. The activation enthalpies for the cleavage reaction in MMSi-Cl and PPSi-Cl are 33.9 and 34.8 kcal/mol, respectively (Table 4). Although an absolute comparison of energies cannot be made between the MMm-Cl and MMSi-Cl compounds, the qualitative trend indicates that the homolytic dissociation of the N_1—Cl bond appears to be rate-limiting over the final cleavage of the Si-alkyl bond. Alkyl cleavage with Cl initially in the α position could also be a viable pathway for the reaction to occur; however, the transition state would require a highly strained three-membered ring and a subsequent hydrogen transfer from C-7 to C-8, or possibly the elimination of H—$Si(OH)_3$ to form a vinyl halide. Probably more likely would be elimination of HCl followed by attack of Cl^- onto Si to produce the silyl chloride and the alkene.

Thus, the present calculations support the current experimental evidence of a Hoffmann-Loeffler style rearrangement that is responsible for the photodecomposition of the N-halamines subjected to UVA light.

In support of these predictions, it is well-known that halogen atoms that are bonded to carbon atoms in alpha or beta positions with respect to a silicon atom are notoriously susceptible to decomposition by C—Si bond scission (33—38). Thus the electron-withdrawing heteroatoms (chlorine in this work) in alkyl side-chains bonded to silicon provide a mechanism for the cleavage of the alkyl groups from silicon as shown in eqs 3 and 4 (33, 36)

$$ClCH_2CH_2SiR_3 \xrightarrow{\Delta} ClSiR_3 + H_2C = CH_2 \qquad (3)$$

$$ClCH_2CH_2SiO_n \xrightarrow[H_2O]{OH^-} Si(OH)_4 + H_2C = CH_2 + Cl^- \qquad (4)$$

Thermally induced cleavage (1) of these compounds can proceed by an intramolecular process resulting in a bond between the silicon and the heteroatom and elimination of ethylene through a four-membered transition state analogous to that shown in Figure 11 (37). On the other hand, the

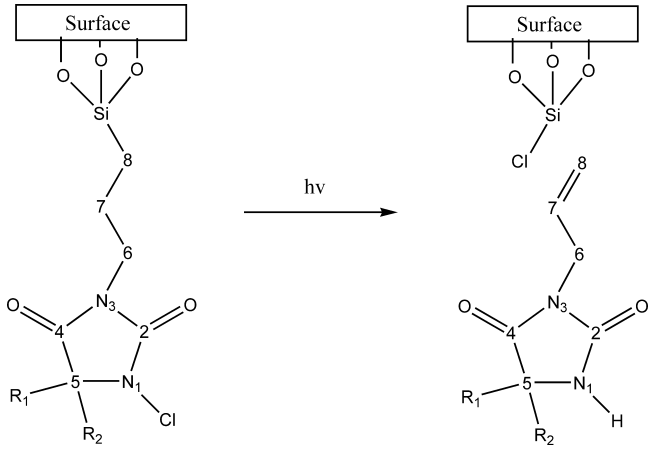

FIGURE 12. Proposed Decomposition of an N-chlorohydantoinylsiloxane.

reaction of siloxane groups with aqueous base can also initiate the elimination of ethylene while breaking the Si—C bond (2) (33, 36). Both mechanisms (1) and (2) could occur during drying or rechlorination of the coated materials (siloxane N-halamine coatings) and cause the cleavage of Si—C bonds resulting in loss of the hydantoin units from the surface of the coated materials, as pictured in Figure 12, and consequently the loss of antimicrobial efficacy of the coated surface.

CONCLUSIONS

A series of hydantoinyl siloxane compounds were coated onto cotton fabric and then treated with bleach to provide an antimicrobial property. The ultraviolet light resistances of the derivatives were compared. Chlorinated coatings decomposed, while unchlorinated coatings did not exhibit any decomposition. Model compounds of the siloxane derivatives were synthesized to investigate the stability of the N—Cl bond and the structures of decomposition products. The decomposition mechanism of the chlorinated siloxane coatings was explained by an intramolecular photorearrangement reaction (Hoffmann—Loeffler rearrangement) followed by cleavage of the alkyl group from the Si atom. Cleavage of the Si—alkyl bond resulted in loss of hydantoin units from the surface of the coated materials. Phenyl substitution at the 5-position of the hydantoin ring did not protect the siloxane coatings from UVA photodegradation.

Acknowledgment. This work was supported by U.S. Air Force through Grant FA8650-07-1-5908.

Supporting Information Available: Additional NMR, FTIR, and GCMS spectra of the compounds and complete computational details (PDF). This material is available free of charge via the Internet at http://pubs.acs.org.

REFERENCES AND NOTES

(1) Kaminski, J. J.; Bodor, N.; Higuchi, T. *J. Pharm. Sci.* **1976**, *65*, 553–557.
(2) Worley, S. D.; Williams, D. E. *CRC Crit. Rev. Environ. Control* **1988**, *18*, 133–175, and references therein.
(3) Sun, G.; Wheatley, W. B.; Worley, S. D. *Ind. Eng. Chem. Res.* **1994**, *33*, 168–170.
(4) Sun, G.; Allen, L. C.; Luckie, E. P.; Wheatley, W. B.; Worley, S. D. *Ind. Eng. Chem. Res.* **1995**, *34*, 4106–4109.
(5) Chen, Y.; Worley, S. D.; Kim, J.; Wei, C. I.; Chen, T. Y.; Santiago, J. I.; Williams, J. F.; Sun, G. *Ind. Eng. Chem. Res.* **2003**, *42*, 280–284.
(6) Sun, G.; Xu, X. *Text. Chem. Colorist* **1998**, *30*, 26–30.
(7) Worley, S. D.; Sun, G. *Trends Polym. Sci.* **1996**, *4*, 364–370, references therein.
(8) Sun, Y. Y.; Chen, T.; Worley, S. D.; Sun, G. *J. Polym. Sci., Part A: Polym. Chem.* **2001**, *39*, 3073–3084.
(9) Chen, Z.; Sun, Y. Y. *Ind. Eng. Chem. Res.* **2006**, *45*, 2634–2640.
(10) Makal, U.; Wood, L.; Ohman, D. E.; Wynne, K. J. *Biomaterials.* **2006**, *27*, 1316–1326.
(11) Coulliette, A. D.; Peterson, L. A.; Mosberg, J. A.; Rose, J. B. *Am. J. Trop. Med. Hyg.* **2010**, *82*, 279–288.
(12) Worley, S. D.; Chen, Y.; Wang, J. W.; Wu, R.; Cho, U.; Broughton, R. M.; Kim, J.; Wei, C. I.; Williams, J. F.; Chen, J.; Li, Y. *Surf. Coat. Int., Part B: Coat. Trans.* **2005**, *88*, 93–100.
(13) Liang, J.; Barnes, K.; Akdag, A.; Worley, S. D.; Lee, J.; Broughton, R. M.; Huang, T. S. *Ind. Eng. Chem. Res.* **2007**, *46*, 1861–1866.
(14) Kocer, H. B.; Akdag, A.; Ren, X.; Broughton, R. M.; Worley, S. D.; Huang, T. S. *Ind. Eng. Chem. Res.* **2008**, *47*, 7558–7563.
(15) Kou, L.; Liang, J.; Ren, X.; Kocer, H. B.; Worley, S. D.; Broughton, R. M.; Huang, T. S. *Coll. Surf. A: Phys. Eng. Asp.* **2009**, *345*, 88–94.
(16) Ren, X.; Akdag, A.; Kocer, H. B.; Worley, S. D.; Broughton, R. M.; Huang, T. S. *Carbohy. Polym.* **2009**, *78*, 220–226.
(17) Kou, L.; Liang, J.; Ren, X.; Kocer, H. B.; Worley, S. D.; Tzou, Y. M.; Huang, T. S. *Ind. Eng. Chem. Res.* **2009**, *48*, 6521–6526.
(18) Salter, B.; Owens, J.; Hayn, R.; McDonald, R.; Shannon, E. *J. Mater. Sci.* **2009**, *44*, 2068–2078.
(19) Sandstrom, A.; Sun, G. *Res. J. Text. Appl.* **2006**, *10*, 13–18.
(20) Kocer, H. B.; Worley, S. D.; Broughton, R. M.; Acevedo, O.; Huang, T. S. *Ind. Eng. Chem. Res.* **2010**, under review.
(21) Becke, A. D. *J. Chem. Phys.* **1993**, *98*, 5648–5652.
(22) Lee, C.; Yang, W.; Parr, R. G. *Phys. Rev.* **1988**, *37*, 785–789.
(23) Frisch, M. J. *Gaussian 09, Revision A.02*; Gaussian, Inc.: Wallingford, CT, 2009 [for full reference, see the Supporting Information].
(24) Ochterski, J. W.; Petersson, G. A.; Montgomery, J. A. *J. Chem. Phys.* **1996**, *104*, 2598–2619.
(25) Droin, A.; Lessard, J. *Tetrahedron Lett.* **2006**, *47*, 4285–4288.
(26) Petterson, R. C.; Wambsgans, A. *J. Am. Chem. Soc.* **1964**, *86*, 1648–1649.
(27) Beckwith, A. L. J.; Goodrich, J. E. *Aust. J. Chem.* **1965**, *18*, 747–757.
(28) Neale, R. S.; Marcus, N. L.; Schepers, R. G. *J. Am. Chem. Soc.* **1966**, *88*, 3051–3053.
(29) Chow, Y. L.; Joseph, T. C. *Chem. Commun.* **1969**, 490–491.
(30) Johnson, R. A.; Greene, F. D. *J. Org. Chem.* **1975**, *40*, 2186–2192.
(31) Darwent, B. D. *Bond Dissociation Energies in Simple Molecules*; National Standard Reference Data Series; National Institute of Standards and Technology: Gaithersburg, MD, 1970; Vol. 31, pp 1—52.
(32) Mo, O.; Yáñez, M.; Eckert-Maksić, M.; Maksić, Z. B.; Alkorta, I.; Elguero, J. *J. Phys. Chem. A* **2005**, *109*, 4359–4365.
(33) Sommer, L. H.; Goldberg, G. M.; Dorfman, E.; Whitmore, F. C. *J. Am. Chem. Soc.* **1946**, *68*, 1083–1085.
(34) Agre, C. L. *J. Am. Chem. Soc.* **1949**, *71*, 300–304.
(35) Kenneth, M. L. U.S. Patent 3 532 733, 1970.
(36) Arkles, B.; Berry, D. H.; Figge, L. K.; Composto, R. J.; Chiou, T.; Colazzo, H.; Wallace, W. E. *J. Sol—Gel Sci. Technol.* **1997**, *8*, 465–469.
(37) Davidson, I. M. T.; Eaborn, C.; Lilly, M. N. *J. Chem. Soc.* **1964**, 2624–2630.
(38) Davidson, I. M. T.; Metcalfe, C. J. L. *J. Chem. Soc* **1964**, 2630–2633.

AM100511X